Region - Water Conservancy, 2026, Volume9, Issue1
DOI: 10.32629/rwc.v9i1.5029
ISSN Online: 2630-4902

Flood assessment using hydraulic modeling in the Burgay River: case study in the El Descanso sector

Sanmartín-Álvarez Brayan Saúl, Prehn-Garcés Claudia, Reyes-Zambrano Jimmy Leandro, Chavarría-Párraga Jesús Enrique
Pontificia Universidad Católica del Ecuador – Manabí Campus. Portoviejo, Ecuador.

Abstract: This study addresses the problem of flooding caused by the overflowing of the Burgay River in the El Descanso sector. Flooding, a growing phenomenon globally due to climate change and urban sprawl, represents a significant threat, causing human and economic losses. In order to identify the areas most vulnerable to this risk, a hydraulic model of a section of the river was carried out using HEC-RAS software. The methodology considered two scenarios. The first represents the current state of the river, while the second simulates the conditions of 1989, when the channel was free of obstructions and accumulated sediment. To feed the model, historical information was collected using satellite imagery, topographic surveys, aerial photographs, and data from the GeoGLOWS Tethys platform. The results of the current scenario reveal that sediment accumulation and human activities increase the magnitude and frequency of floods. In contrast, the 1989 scenario shows a significant improvement in the river's capacity to handle high flows, which positively affects flow dynamics. Furthermore, the generated flood maps are crucial tools for planning and risk management in the region. Finally, the implementation of monitoring stations at strategic points is proposed to obtain more accurate data that will allow for the optimization of mitigation and response strategies to flood events.

Key words: modeling; sediments; flooding

1 Introduction

Throughout history, flooding has been a recurring phenomenon, primarily caused by river overflows, heavy rainfall, and snowmelt (Ordoñez, 2015). In response, early societies developed drainage systems and canals as mitigation measures. Over time, these solutions evolved into more advanced infrastructure such as dikes and dams. However, rapid urbanization, population growth, and climate change have significantly increased the risk of flooding, especially in densely populated urban areas, as noted by the Organization of American States (OAS, 1993). Human interventions, such as soil sealing, have reduced natural infiltration capacity, increasing surface runoff and exacerbating the problem.

In recent decades, floods have caused considerable human, economic, and environmental losses. It is estimated that approximately 50% of climate disasters are water-related, causing around 1.3 million deaths in the last fifty years (UN-Habitat, 2021; Salazar, 2018). This increasing frequency and magnitude of floods underscores the need to implement more effective risk management strategies adapted to the current context.

Integrated flood management requires a combination of approaches, including sustainable urban planning, watershed management, the implementation of early warning systems, and the improvement of control infrastructure (Bello et al.,

2020). Furthermore, promoting wetland conservation and the restoration of natural ecosystems are essential to reducing the impact of flooding, along with the development of community-based contingency plans (Royal et al., 2018).

In this context, hydraulic modeling has proven to be a crucial tool for the analysis and prediction of flood events. Zambrano (2020), for example, used HEC-RAS software to analyze a section of the El Chorro stream, obtaining positive results in the simulation of scenarios. Similarly, Timbe and Timbe (2012) used this software to map flood hazard in mountain rivers, demonstrating its accuracy in scenarios with limited data.

This study focuses on the El Descanso sector, on the border of the Azuay and Cañar provinces of Ecuador. The area is traversed by the Burgay River and has been affected by several flooding events in recent years. A significant example was the 2021 event, which caused severe damage to public and private infrastructure, including the collapse of important roads (SNDGR, 2021).

This study focuses on the El Descanso sector of the Burgay River in Ecuador, an area vulnerable to recent flooding that has caused significant damage (SNDGR, 2021). Using HEC-RAS, the hydraulic behavior of the river will be analyzed under two scenarios: its current state and a simulation based on 1989 conditions. The objective is to identify the areas of greatest risk and develop flood maps to facilitate risk management in the region.

2 Materials and methods

A quantitative research approach was used for the development of this study. This approach is based on the collection and analysis of numerical data, which not only seeks to understand the flooding pattern but also to propose strategies for flood risk management in the study area.

2.1 Location

The study area was in the El Descanso sector (Cuenca, Azogues and Paute cantons), corresponding to a section of the Burgay River, from the confluence of the Déleg and Burgay rivers, point with UTM WGS84 zone 17S coordinates: X:735593.54 Y:9687131.35; to the confluence with the Tomebamba River, point with UTM WGS84 zone 17S coordinates: X: 736451.53 Y: 9686119.55; with a length of 1436.74 m

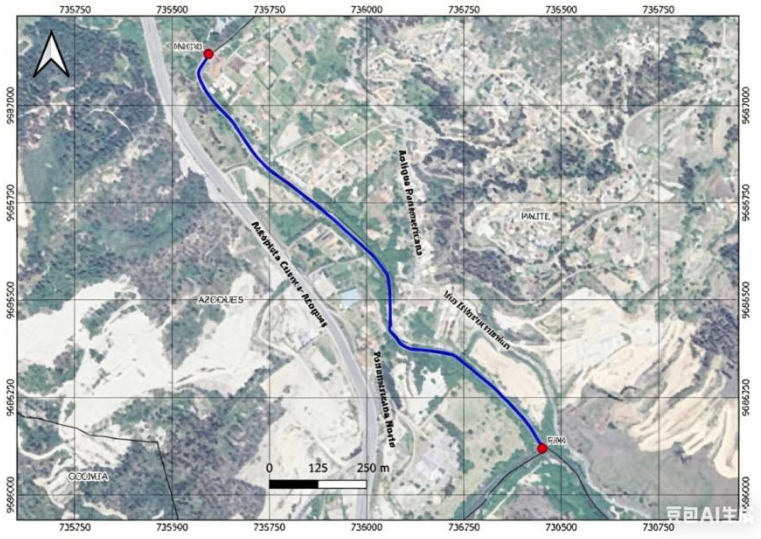

Figure 1. Map of the section of the Burgay River chosen for the study

2.2 Hydraulic study

2.2.1 Hydraulic modeling

Hydraulic modeling is defined as the process of simulating phenomena and processes associated with water flow (Stenta et al., 2018). It is a deterministic method based on pre-established physical principles, which can be based on

general concepts of two-dimensional analysis or on the use of empirical equations for specific processes. It is crucial that the physical and hydrodynamic parameters of the model accurately represent real-world magnitudes according to specific laws, known as scales (Morresi et al., 2018). These magnitudes include physical properties such as water velocity and flow depth, and the scales allow these characteristics to be represented precisely in the model. The accuracy of the results depends on the appropriate use of these scales. However, some aspects cannot be accurately represented in the model, generating scale effects.

2.2.2 Hydraulic modeling tool selection

Various hydraulic modeling tools exist, including dimensionless, one-dimensional, two-dimensional, and three-dimensional options. Each is suitable for different scenarios or case studies (Khaled, 2008). In this study, the Hydrological Engineering Center – River Analysis System (HEC-RAS) software, developed by the U.S. Army Corps of Engineers, was used. This software is freely available. A significant advantage of HEC-RAS is that it requires a limited amount of data to obtain accurate and representative results (Timbe and Timbe, 2012).

2.2.3 Design flow rate

The flow rate for the model was obtained through the GeoGLOWS Tethys platform, available on the portal of the National Institute of Meteorology and Hydrology (INAMHI) as we observe in Figure 2, in collaboration with the EcoCiencia Foundation and the International Center for Tropical Agriculture (CIAT), under the SERVIR-Amazonia program, which is part of SERVIR Global, a joint initiative of NASA and the United States Agency for International Development (USAID), among others (INAMHI, 2022).

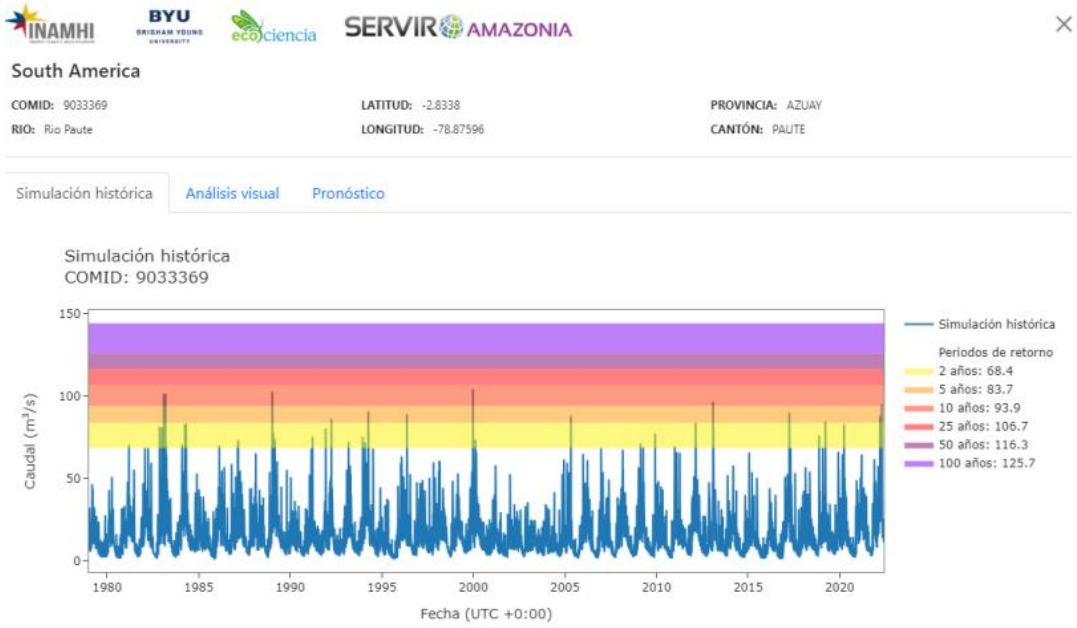

Figure 2. Data visualization environment on the GeoGLOWS platform

To validate the data, they were compared with those used by Timbe and Timbe (2012), who modeled a section of the Burgay River upstream of the study area. This author estimated flood flows using results from the study by Estrella and Tobar (1994), who established maximum flows for return periods of 10, 20, and 50 years at points on the Burgay and Deleg rivers, using data from the Tomebamba station, which has reliable flow records for 23 years (1964–1987).

Table 1. Comparison of flow rates obtained from the GeoGLOWS platform and the study by Luis and Edison Timbe

Return Period TR	GeoGLOWS (m^3/s)	Luis T & Edison T (2012) (m^3/s)
25 years	106.7	97.5
50 years	116.3	110.8
100 years	125.7	124.2

2.3 Topographic information

Topography is a crucial element in hydraulic modeling, as its accuracy determines the reliability of the results obtained. In this study, a Digital Terrain Model (DTM) was generated from topographic data collected by the Ministry of Water, Environment and Ecological Transition (MAATE), which included a detailed review of cross-sections, infrastructure, floodplains, and bathymetry (Figure 3). This data was supplemented with a photogrammetric survey (Figure 4). Subsequently, the topographic information was processed, and the DTM was created using QGIS software (Figure 5).

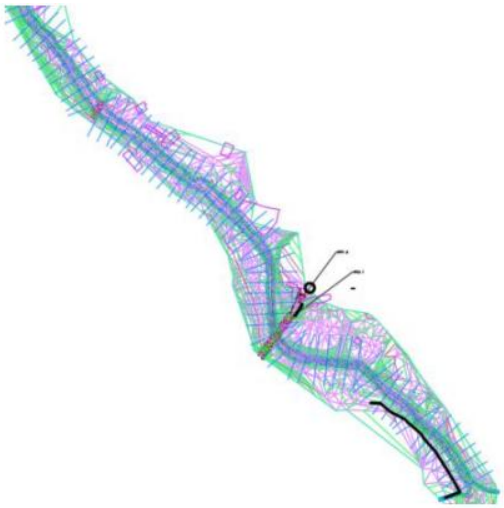

Figure 3. Topographic survey visualized in Civil 3D

Figure 4. Photogrammetric survey of the river section under study

The topography was studied considering the references of the surveyed points, in addition to aerial photographs

belonging to the IGM from 1989, where it was possible to determine the width of the river channel for that time, trying to generate the topographic conditions that simulate the free flow of sediments and obstructions currently existing, which was called scenario two.

The image below shows the work done in the study area.

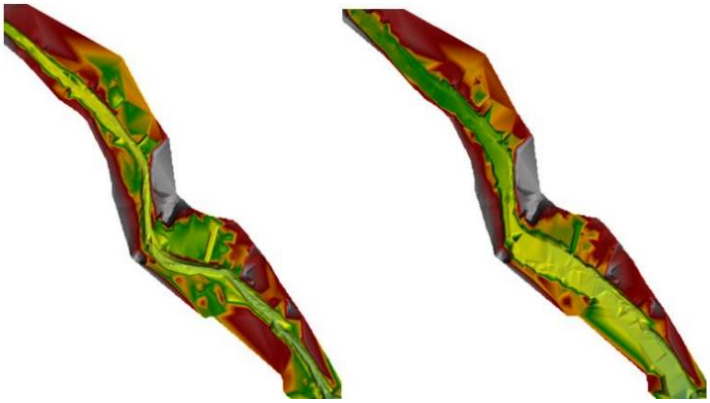

Figure 5. The current terrain topography is shown on the left, and the edited topography simulated to its 1989 state is shown on the right.

2.4 Geometry

The "RiverGis" plugin, an extension of the free software QGIS, was used to construct the model geometry. This plugin allows for the preparation of detailed geometric data and its subsequent export to the HEC-RAS model. The geometry considered included:

• Banklines: represent the lateral edges of the river.

• Stream Centerline: defines the main axis of the flow.

• Flowpaths: These indicate the routes the water follows.

• SxCutlines (transverse sections): were generated every 30 meters, with a total of 47 sections, each having a width of 120 meters.

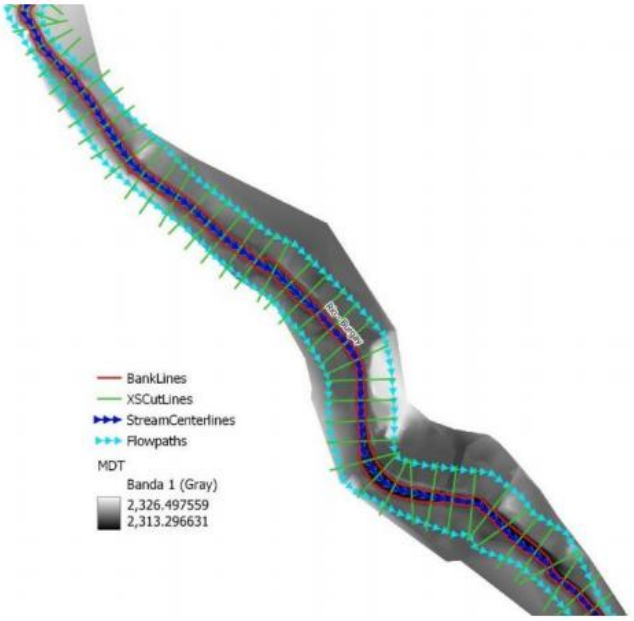

Figure 6. Geometry generated with River Gis.

2.5 Infrastructure

The bridge located in the El Descanso sector is a crucial element in the study area, as it connects the southern region with the eastern region. Detailed measurements were taken to represent it in the model, considering the bridge's dimensions, such as length and width, the height and width of the arches, and the spacing between them. These measurements were processed in Excel to obtain the bridge's profile in terms of elevation and abscissa, and were then incorporated into the HEC-RAS model, indicating the distance of the infrastructure both upstream and downstream from the nearest cross-section (Figures 7 and 8).

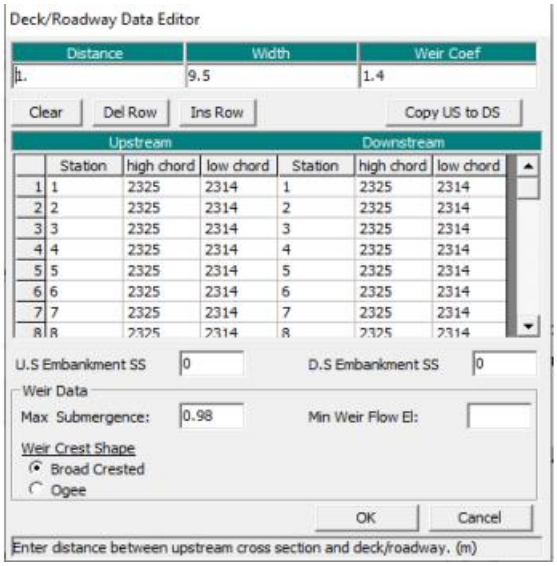

Figure 7. Infrastructure data entered into the model.

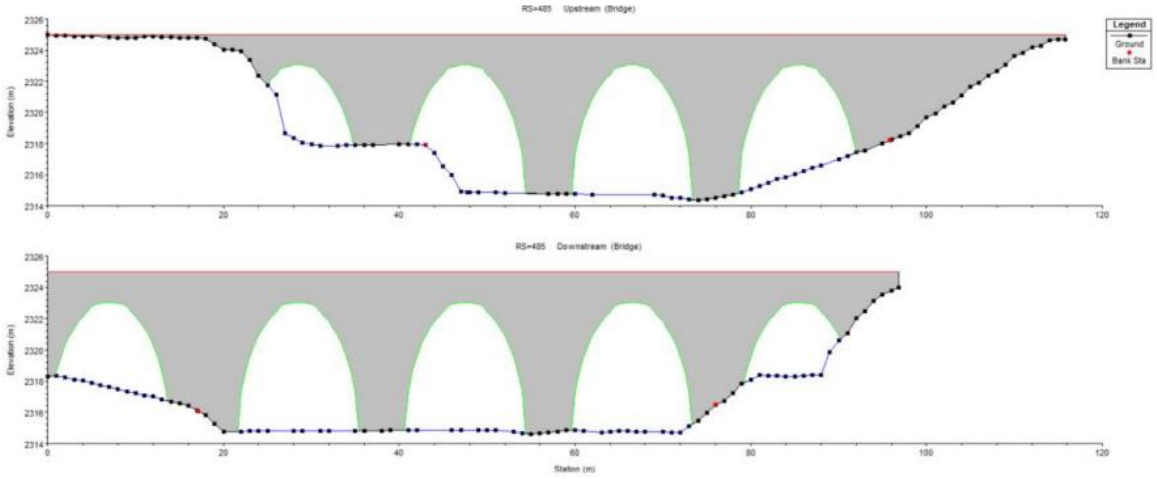

Figure 8. Detail of the bridge included in the HEC-RAS model.

2.6 Roughness coefficient

The roughness coefficient depends on factors such as surface, vegetation, material, and terrain irregularities (Bustamante et al., 2023). Since there is no exact method for determining it, a field inspection was conducted, and Chow's table (1994) was used as a reference. An average value of n=0.040 was estimated for the riverbed due to the presence of uniform rocks and gravel. For the floodplains, a value of n=0.030 was assigned, considering the predominant vegetation and material.

2.7 Contraction and expansion coefficients

These coefficients measure the energy losses during the transition between consecutive cross-sections. According to

Timbe and Willems (2011), a contraction coefficient of 0.1 was established, indicating a 10% loss of kinetic energy as the flow contracts, and an expansion coefficient of 0.3, representing a 30% loss as it expands. These values were based on the HEC-RAS software manual.

2.8 Boundary conditions

A supercritical flow was defined, with a normal depth and a representative upstream slope, as these conditions best reflect the river's characteristics. The selection was made after analyzing topographic, hydraulic, and geometric aspects of the study area.

3 Results and discussion

The model considered the same factors and criteria for both scenarios, with the riverbed topography being the only differentiating variable. It is important to note that this topographic modification was made after analyzing current hydraulic conditions and historical records, concluding that the sediment characteristics do not present significant variations that would justify a modification of the Manning coefficient. This is key, since the main objective is to evaluate how topography affects river behavior. While it is true that changing various variables could influence the model's results, in this case, the aim was to isolate the specific impact of topography.

3.1 Determination of the hydraulic behavior in the study section, considering the current topography of the river

The results of the HEC-RAS model were used to simulate scenario one, which represents the current state of the river, considering different return periods of 25, 50 and 100 years.

3.2 Numerical results

Table 2 provides a representative sample of these results. The main hydraulic parameters obtained from this analysis include:

Total discharge (Q Total), minimum channel bed topographic elevation (Min Ch El), water surface elevation (W. S. Elev), critical depth elevation (Crit W. S), energy grade elevation (E. G. Elev), energy grade slope (E. G. Slope), channel center velocity of the cross section (Vel Chnl), wetted area (Flow Area), water surface top width (Top Width), and section Froude number (Froude # Chl).

Table 2. Numerical results from section 1,410 for the different return periods

Profile	Q Total m^3/s	Min Ch El m	W.S. Elev m	Crit W.S. m	E.G. Elev m	E.G. Slope m/m	Vel Chnl m/s	Flow Area m^2	Top Width m	Froude # Chl
TR 100	125.7	2320	2322.1	2321.8	2322.5	0.00597	2.94	44.96	30.23	0.68
PF 50	116.3	2320	2322.0	2321.7	2322.4	0.00663	2.96	41.16	29.61	0.7
PF 25	106.7	2320	2321.8	2321.6	2322.3	0.00731	2.97	37.5	28.5	0.73

It has been shown that, for a 100-year return period, higher values are obtained for flow rate, water level rise, energy line elevation, and flow area compared to other return periods. However, in the case of a 25-year return period, the highest values are observed for energy grade slope, flow velocity, and Froude number.

3.3 Water levels in cross sections

The behavior of the water level in section 600 is detailed below:

- 100-year return period: the water level reaches an elevation of 2,322.13 m.
- 50-year return period: the water level reaches 2,322.01 m.
- 25-year return period: the water level reaches 2,321.88 m.

Although the differences between the 100 and 50 year return periods are minimal, a more significant variation is seen

when comparing these with the 25 year return period.

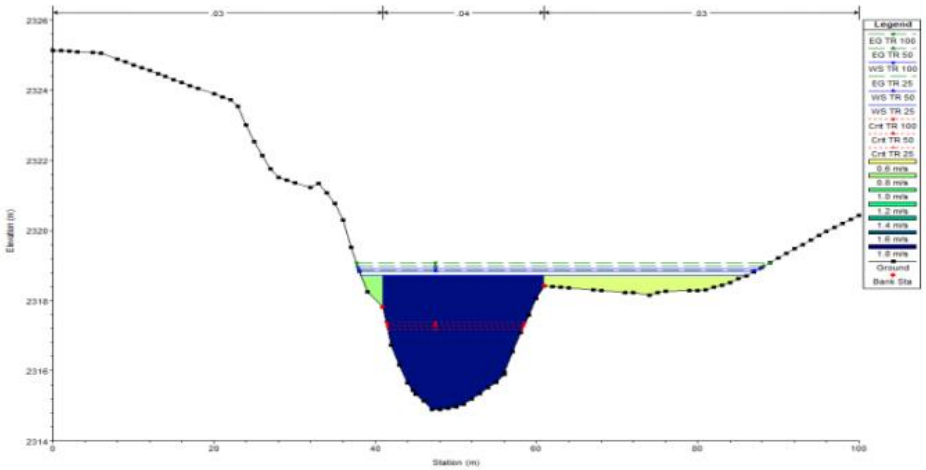

Figure 9. Results of the free surface water level for the different return periods in section 600.

3.4 Water level in the infrastructure

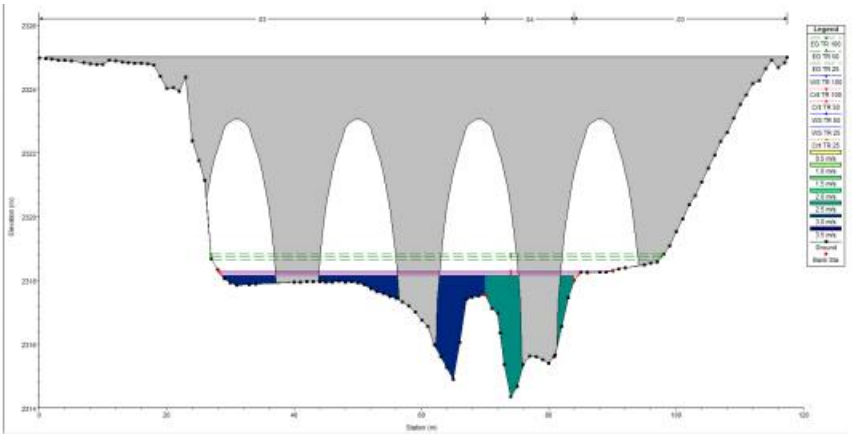

Figure 10. Upstream bridge

We identified that upstream of the bridge, the maximum water level reaches elevation 2318.1

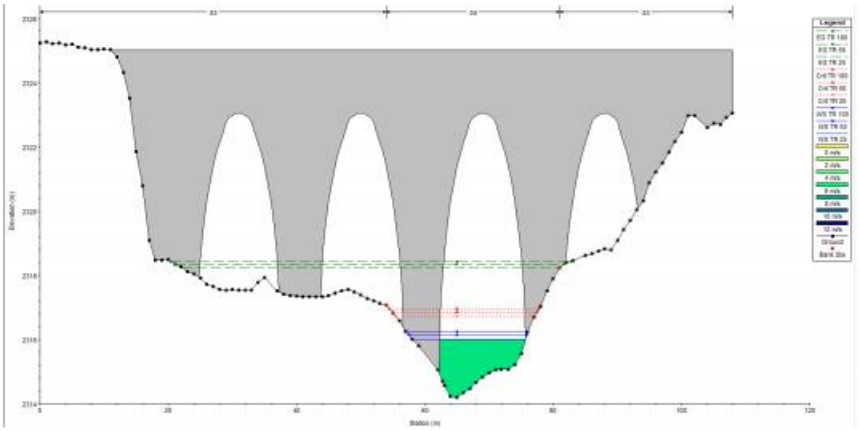

Figure 11. Downstream bridge

Downstream of the bridge, the maximum water level reaches an elevation of 2,316.02 m, which is 2 meters lower than the water level upstream of the bridge.

3.5 Longitudinal profile of the study section

The following figure shows the results obtained along the longitudinal profile, where the water levels corresponding

to the return periods of 25, 50 and 100 years are visualized.

The longitudinal profile is not uniform, with a notable variation in the area where the bridge is located. It is important to highlight that upstream of the bridge, there is a significant rise in water level, while downstream there is a significant decrease. This behavior directly influences key variables such as flow velocity and system energy.

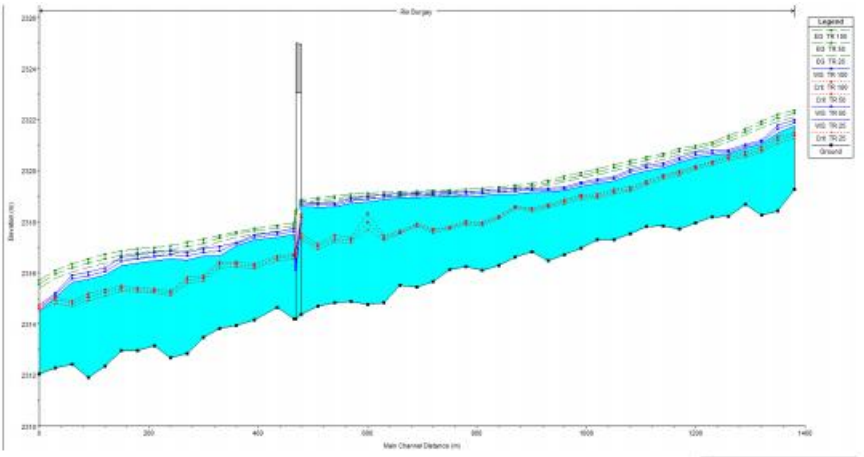

Figure 12. Longitudinal profile with water levels at different return periods.

The results obtained with the model for scenario two "simulated state with the riverbank free of obstacles" are presented.

3.6 Numerical results

Annex 4 compiles the numerical results for all analysed cross sections, while Table 2 presents a sample of these results. The hydraulic calculation yields the following parameters: total discharge (Q Total), minimum channel bed topographic elevation (Min Ch El), water surface elevation (W. S. Elev), critical depth elevation (Crit W. S), energy grade elevation (E. G. Elev), energy grade slope (E. G. Slope), central channel velocity of the cross section (Vel Chnl), wetted area (Flow Area), top width (Top Width), and section Froude number (Froude # Chl).

Table 3. Numerical results of section 1410 for the different return periods.

Profile	Q Total m^3/s	Min Ch El m	W.S. Elev M	Crit W.S. m	E.G. Elev m	E.G. Slope m/m	Vel Chnl m/s	Flow Area m^2	Top Width m	Froude # Chl
TR 100	125.7	2319.26	2321.97	2321.4	2322.3	0.0047	2.79	47.48	29.45	0.61
TR 50	116.3	2319.26	2321.86	2321.3	2322.2	0.0050	2.78	44.03	29.04	0.62
TR 25	106.7	2319.26	2321.74	2321.2	2322.1	0.0052	2.74	40.66	28.55	0.63

The results obtained are similar to those of the first scenario. It is found that discharge, water surface elevation, energy grade elevation and flow area increase as the return period rises; however, the water level elevations are lower compared with the first scenario.

3.7 Water level in cross-sections

The image below details the levels obtained for section 600.

The water level with a return time of 100 years we observed reaches the elevation of 2,321.97 m, with 50 years it reaches 2,321.86 m and for 25 years it reaches 2,321.74 m.

The behavior of the water level in section 600 is detailed below:

- 100-year return period: the water level reaches an elevation of 2,321.97 m.

- 50-year return period: the water level reaches 2,321.86 m.
- 25-year return period: the water level reaches 2,321.74 m.

It is clear that the differences between TR 100 and TR 50 are not marked, however, with a TR 25 a difference is already noticeable.

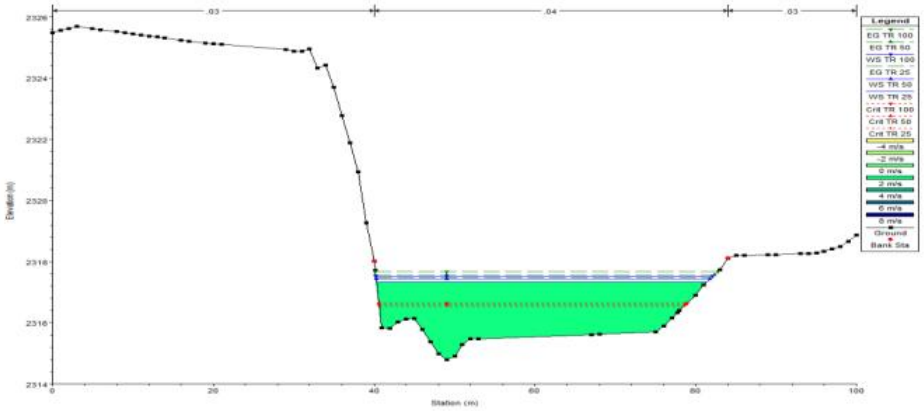

Figure 13. Results of the free surface water level for the different return periods in section 600.

3.8 Water level in the infrastructure

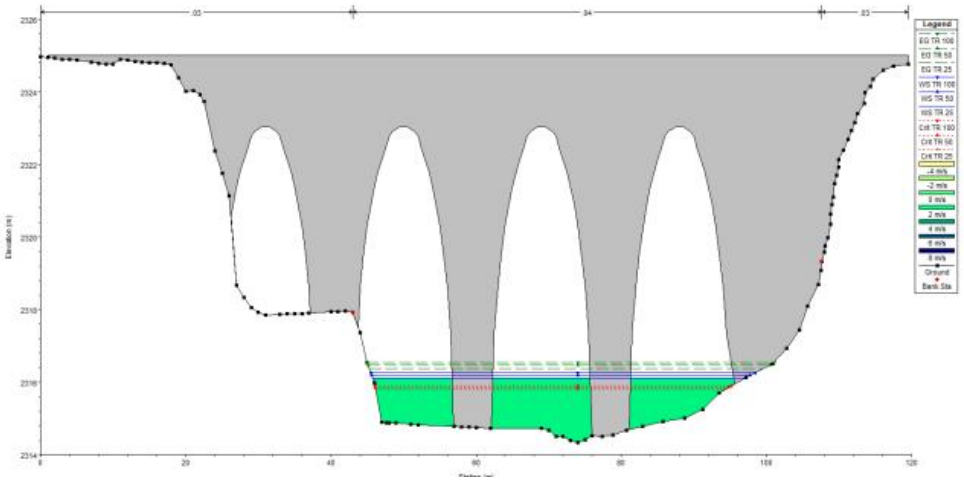

Figure 14. Upstream bridge

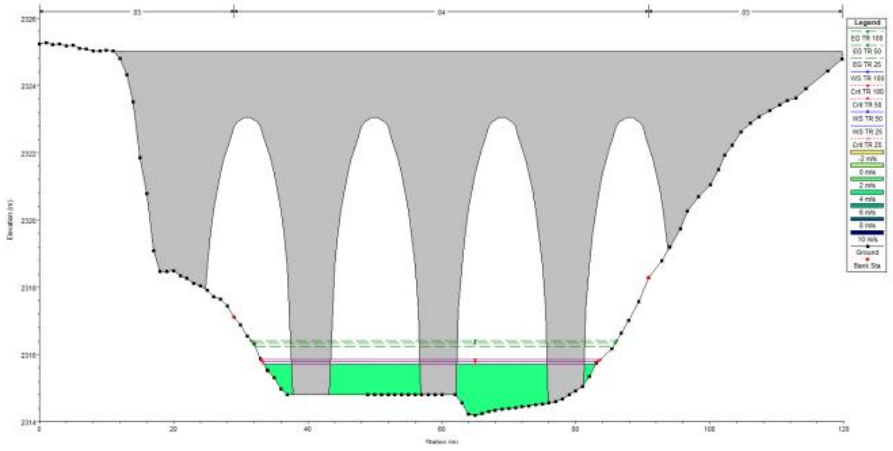

Figure 15. Downstream bridge

As a result, the water level at the bridge upstream reaches an elevation of 2,316.1m and downstream an elevation of 2,315.8m. The difference is minimal, indicating no alteration in the water flow.

3.9 Longitudinal profile of the study section

The following figure presents the results obtained along the longitudinal profile, in which the water levels for the different return periods can be observed: 25, 50 and 100 years return.

We found that the longitudinal profile is uniform, since there is no alteration in the area where the bridge is located; therefore, there is no impact on speed and energy.

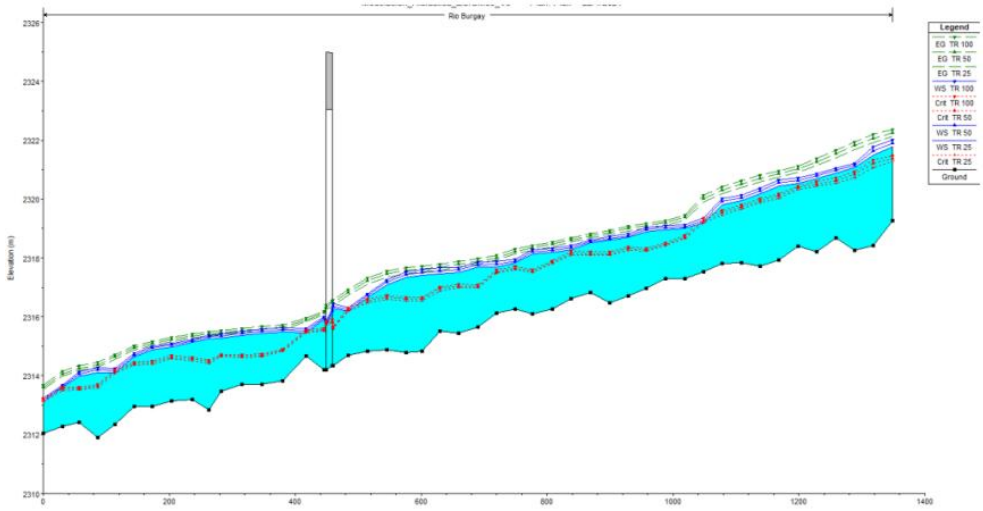

Figure 16. Longitudinal profile with water levels at different return periods.

Figure 17. On the left, flood patch with scenario one and on the right, flood patch with scenario two, for a 50-year return period

3.10 100-year return period

For Scenario One, more extensive river channel overflow is observed, affecting a larger area compared with the 25-year return period, including urban zones and infrastructure. In Scenario Two, the river flow remains stable and confined within its channel without causing overtopping.

Figure 18. On the left, flood patch with scenario one and on the right, flood patch with scenario two, for a 100-year return period

In a recent study focused on the Burgay River, Idrovo (2024) revealed that the critical infrastructure of the Biblián Canton is in an alarming state. 31% of the drinking water network, 45% of the sewage system, 44% of urban roads, and a worrying 67% of bridges are exposed to a very high or high risk of flooding. These findings underscore the urgent need to implement preventative measures and risk management strategies to protect public health and the local economy from extreme weather events.

4 Conclusion

Hydraulic modeling revealed that critical sediment accumulation zones and human intervention have significantly altered the flow of the Burgay River, increasing its susceptibility to flooding. This is especially evident in areas where the channel narrows, increasing the water level during flood events and creating a high risk of overflow.

The bridge in the El Descanso sector is one of the most affected areas, with only one of its arches functioning properly due to sediment buildup. This situation drastically alters the flow dynamics, increasing the risk of flooding in the area.

Historical analysis showed that when the river channel was wider and free of obstructions, water levels during floods were significantly lower. This suggests that restoring the original channel could considerably reduce the risk of flooding and improve the river's capacity to handle high flows, especially affecting critical infrastructure such as the bridge.

Finally, the flood maps generated for the two scenarios and different return periods are fundamental tools for urban planning and watershed management. These maps allow for the implementation of more effective mitigation and prevention measures, contributing to better disaster risk management in the region.

Conflicts of interest

The author declares no conflicts of interest regarding the publication of this paper.

References

[1] Bello, O., Bustamante, A., & Pizarro, P. (2020). Planificación para la reducción del riesgo de desastres en el marco de la Agenda 2030 para el Desarrollo Sostenible (Institucional, M1-32BTS- 000130). Oficina de la Secretaría de la Comisión Económica para América Latina y el Caribe. https://repositorio.cepal.org/server/api/core/bitstreams/26f2977e-45ae-4fe0-9864-e52c63189100/content

[2] Bustamante, M. C. R., Castro, L. M.T., & Parra, L. V. C. (2023). Sensibilidad del coeficiente de Manning en la estimación de los niveles de crecida para el mapeo de inundaciones en un río de la región interandina de Ecuador. Cuadernos de Geografía: Revista Colombiana de Geografía, 32(1), 118-129. https://doi.org/10.15446/rcdg. v32n1.94764

[3] Chow, V. (1994). Hidráulica de canales abiertos (2.a ed., Vol. 1). Editorial Martha Suáres R. https://webooks.co/images/team/academicos/ingenieria/civil/11.Hidraulica%20de%20Canales%20Abiertos%20%20Ven%20Te%20Chow.pdf

[4] Idrovo Ortiz, J. P., Paucar Camacho, J. A., & aibor Velasco, N. I. (2024). Análisis de riesgo de inundación en áreas aledañas al río Burgay en la ciudad de Biblián. ConcienciaDigital, 7(1.3), 113-133.

https://doi.org/10.33262/conci enciadigital.v7i1.3.2941

[5] IGM. (1989). Fotografía aérea. Cartografía disponible en: https://www.geoportaligm.gob.ec/

[6] INAMHI GEOGLOWS. (2022). Portal de acceso, visualización y descarga pronósticos hidrometeorológicos e información satelital en Ecuador. [Institucional]. INAMHI GEOGLOWS.https://inamhi.geoglows.org/

[7] Khaled Mohames, A. H. (2008). Aplicaciones del modelo HEC-RAS para el análisis del flujo no permanente con superficie libre [Tesis de masterado, Escuela Politécnica Nacional]. Repositorio de la EPN. http://bibdigital.epn.edu.ec/handle/15000/846

[8] MTOP. (2022). MTOP articula acciones por desbordamiento del río Burgay – Ministerio de Transporte y Obras Públicas [Gubernamental]. Comunicados. https://www.obraspublicas.gob.ec/mtop-azuay-articula-acciones-por-desbordamiento-del-rio- burgay/

[9] Morresi, M. del V., Marcus, R., Gardiol, M., & Biancotti, E. (2018). Modelación hidrológica hidráulica con información de actores sociales en la cuenca del arroyo Las Turbias, Santa Fe Argentina. Aqua-LAC, 10(2), 46-60. https://doi.org/10.29104/phi- aqualac/2018-v10-2-05

[10] Ordoñez Criollo, K. L. (2015). Diagnóstico de la situación Actual del muelle de Cabotaje de la parroquia de Puerto Bolívar por inundaciones en Pleamar [Tesis de masterado, Universidad Técnica de Machala]. Repositorio de la UTMH. http://repositorio.utmachala.e du.ec/handle/48000/5609

[11] ONU-Habitat. (2021). Sequías, tormentas e inundaciones: El agua y el cambio climático dominan la lista de desastres. https://onu-habitat.org/index.php/sequias-tormentas-e-inundaciones- el-agua-y-el-cambio-climatico-dominan-la-lista-de- desastres

[12] OEA. (1993). Manual Sobre el Manejo de Peligros Naturales en la Planificación para el Desarrollo Regional Integrado [Institucional]. Una Contribución al Decenio Internacional para la Reducción de Desastres Naturales. https://www.oas.org/DSD/pub lications/Unit/oea65s/begin.ht m#Contents

[13] Royal, C., Finlanson, C., Siobhan, F., Darwall, W., Dema, M., Parennou, C., & Stroud, D. (2018). Perspectiva mundial sobre los humedales: Estado de los humedales del mundo y de los servicios que prestan a las personas 2018 [Organizacional]. Ramsar convención sobre los humedales. https://www.ramsar.org/sites/ default/files/flipbooks/ramsar_gwo_spanish_web.pdf

[14] Salazar Briones, C., Hallack Alegría, M., Mungaray Moctezuma, A., Lomelí, M. A., Lopez Lambraño, A., Salcedo Peredia, A., Salazar Briones, C., Hallack Alegría, M., Mungaray Moctezuma, A., Lomelí, M. A., Lopez Lambraño,A., & Salcedo- Peredia, A. (2018). Modelación hidrológica e hidráulica de un río intraurbano en una cuenca transfronteriza con el apoyo del análisis regional de frecuencias. Tecnología y ciencias del agua, 9(4), 48-74. https://doi.org/10.24850/j-tyca-2018-04-03

[15] SNDGR. (2021). El Sistema Nacional Descentralizado de Gestión de Riesgos se activa debido a inundación en El Descanso – Secretaría Nacional de Gestión de Riesgos. Gubernamental. https://www.gestionderiesgos. gob.ec/el-sistema-nacional-descentralizado-de-gestion- de-riesgos-se-activa-debido- a-inundacion-en-el-descanso/

[16] Stenta, H., Riccardi, G., Basile, P., & Scuderi, C. (2018). Modelación matemática hidrológica-hidráulica del

escurrimiento superficial en la cuenca del A Pavón (Santa Fe, Argentina). Cuadernos del CURIHAM, 24, 11-23. https://doi.org/10.35305/curih am.v25i0.122

[17] Timbe, L., & Timbe, E. (2012). Mapeo del peligro de inundación en ríos de montaña, caso de estudio del río Burgay. Maskana, 3(1), Article 1.https://doi.org/10.18537/mskn.03.01.07

[18] Timbe, L., & Willems, P. (2011). Desempeño de modelos hidráulicos 1D y 2D para la simulación de inundaciones. Maskana, 2(1), Article 1. https://doi.org/10.18537/mskn.02.01.06

[19] Zambrano, X. (2020). Estudio Hidrológico ─ Hidráulico, de un tramo de la quebrada "El Chorro" en el sector de Ucubamba [Tesis de grado, Universidad del Azuay]. Repositorio de la UA. https://dspace.uazuay.edu.ec/handle/datos/10259